Pierre Touzelet
E-mail : p.touzelet@orange.fr

Hessel's Anna amplifier

Model and results of simulations

Document change record

Date	Issue n°	Pages affected	Comments	Status
17/05/14	1	All	First release of the document.	Preliminary
26/05/14	2	All	Precise location and connection of the floating HT supplies, as required for the Parallel Push-Pull. Addition of a photo of the Hessel's Anna Amplifier	Final
27/05/14		Page 3 Page 7 and Pages 15-20	Update of the driver stage schematic diagram Annex 1 suppressed	Final

1 Objectives

During the amplifiers contest, between students of the Tube Society, held on May 10, 2014, at the Menno van der Veen 's new laboratory, in Hitchum, The Netherlands, we found the Hessel's Anna amplifier interesting for its excellent sounding and its Parallel Push-Pull using KT88 beam tetrodes, triode connected. It appeared rapidly that, this amplifier was certainly the basis of a future excellent amplifier so, back home, we decided to set-up a complete model of this amplifier, as designed by Mr Hessel, to evaluate objectively its performances through simulations and detect eventually, points that should be revisited.

2 Schematic diagram and notations

The following schematic diagrams are based on the Hessel's one, defined on the drawing Hessel Haagsma PEOHH-Project 2013-V4.
They allow identifying strictly nodes and branches of the network as well as components involved.
The different supply voltages are defined by ideal voltage source that behave for AC as short-circuits. Hence, filtering sections have not been represented.

2.1 Driver section

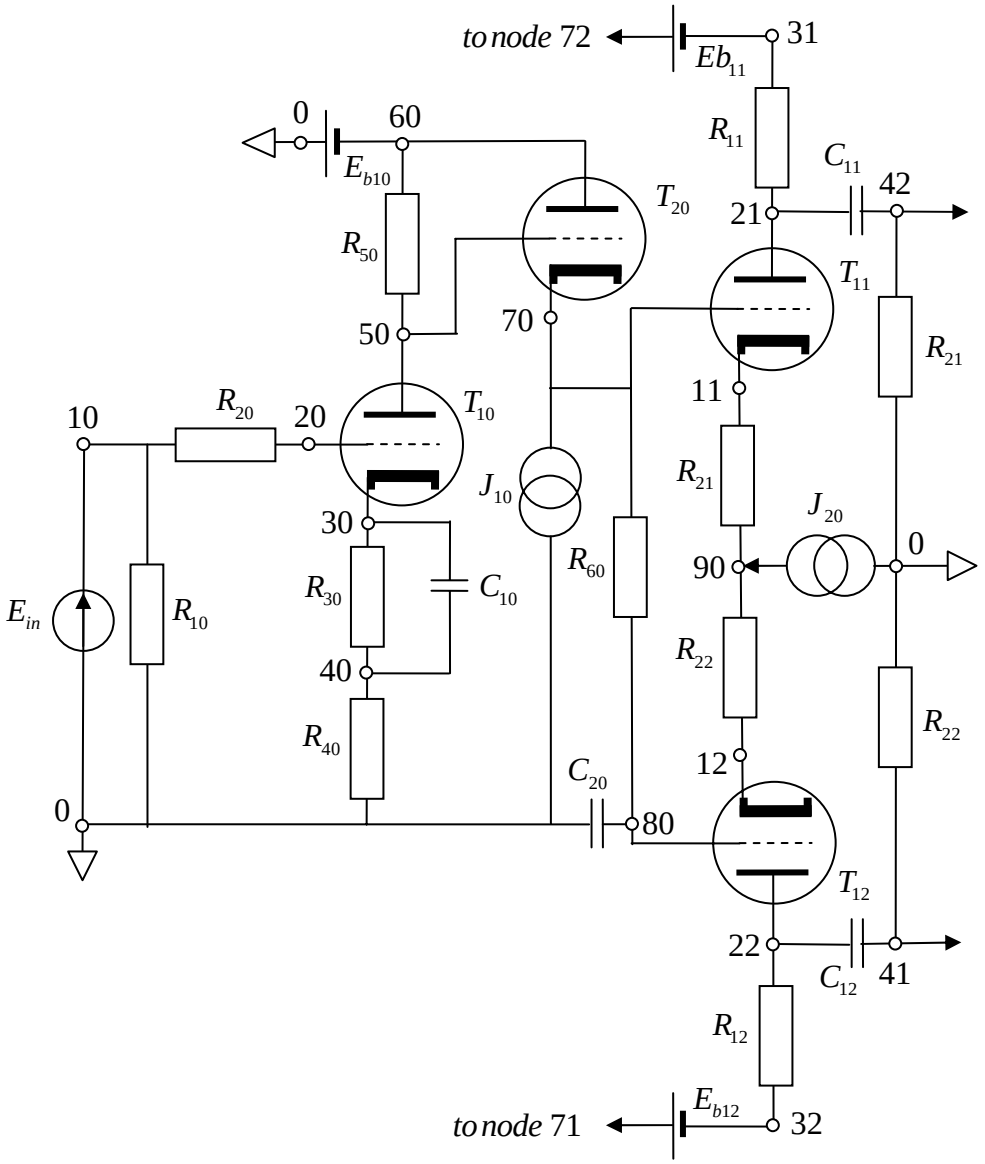

2.2 Power section

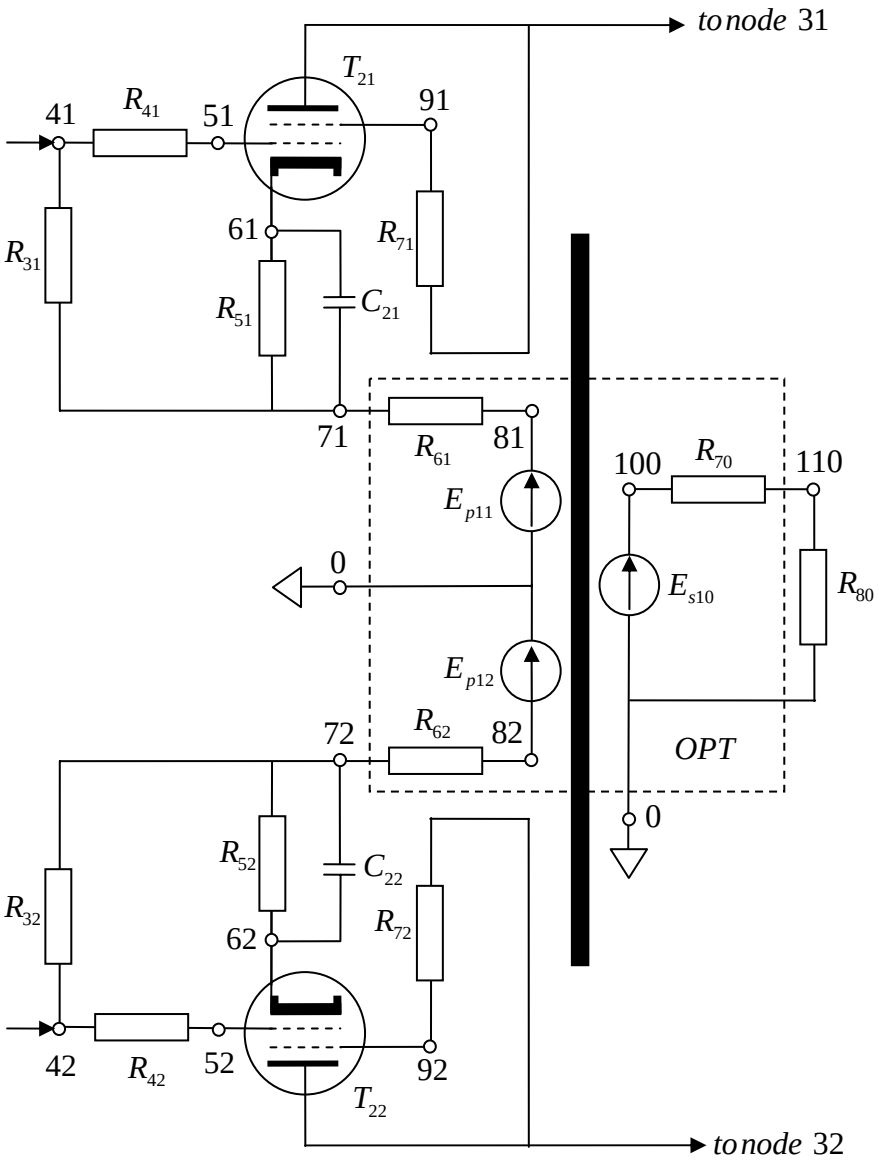

Remark

The feedback loop is not indicated on above schematic diagrams because, not considered in our analysis. Later, if necessary, it can be easily added to the model.

3 Model of particular components

3.1 Triodes

Triodes are modeled using a set of 5 fitting parameters t_1, t_2, t_3, t_4, t_5,along with the following equations:

$$E_1 = \frac{V_{ak}}{t_1} LN\left[1 + Exp\left[t_1\left[\frac{1}{t_2} + \frac{V_{gk}}{\left(t_3 + V_{ak}^2\right)^{\frac{1}{2}}}\right]\right]\right]$$

If $E_1 > 0$

Then

$$I_a = \frac{E_1^{p_4}}{p_5}$$

Else

$$I_a = 0$$

Parameter values used for the triode type ECC88 and 6CG7 are given in the following table:

	t1	t2	t3	t4	t5
ECC88	256	31,9	435	1,22	109
6CG7	165	21,2	1710	1,3	667

3.2 Beam tetrodes

The beam tetrodes are modeled using a set of 5 fitting parameters: p_1, p_2, p_3, p_4, p_5 along with the following equations:

$$\alpha = \frac{2}{\pi} Arctg \frac{V_{ak}}{p_5}$$

$$E_1 = \frac{V_{g_2k}}{p_1} LN\left[1 + Exp\left[p_1\left[\frac{1}{p_2} + \frac{V_{gk}}{V_{g_2k}}\right]\right]\right]$$

IF $E_1 > 0$

Then

$$I_a = \frac{E_1^{p_3}}{p_4}\alpha \qquad I_{g_2} = \frac{E_1^{p_3}}{p_4}\left[1-\alpha\right]$$

Else

$$I_a = 0 \qquad I_{g_2} = 0$$

Parameter values used for the beam tetrodes type KT88 are given in the following table:

	p1	p2	p3	p4	p5
KT88	548	5,655	2,168	11810	23,93

Remark

Above models are those proposed by Norman L. Koren. They are only valid for negative control grid. If they are accurate enough for triodes, they are less good for beam tetrodes. We have nevertheless used them because, beam tetrodes, in the particular case of the Hessel's Anna amplifier, are working, triode connected, with a large amount of local negative feedback, making equivalent tubes much less dependent of their own characteristics.

3.3 OPT core

The core material of the OPT is of the GOSS type and its relative permeability is given using the following equations:

$$\mu_{cr} = 1 + \frac{b}{H_c}\left[\coth\left(aH_c\right) - \frac{1}{aH_c}\right]$$

$$a = a_{\min} + (a_{\max} - a_{\min})th\left|cH_c\right|$$

Where:

$a_{\min}$	1,2E-02
$a_{\max}$	8,9E-02
b	1,67E06
c	6,2E-02

The magnetic circuit is modeled according to the following schematic diagram and equations:

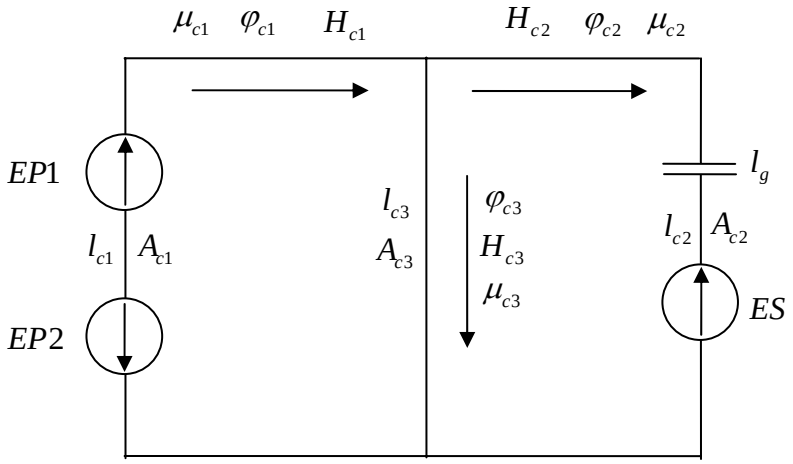

$A_{c1} = A_{c2} = A_{c3} = A_c$	Core cross section
l_c	Average magnetic path length
l_g	Parasitic air gap
$l_{c_1} = l_{c_2} = \frac{l_c}{2}$	Average partial magnetic path length
$\mu_{c_3} = \mu_0$	Free space permeability
$EP1 = \frac{Np}{2}\left(I_{a_{01}} + i_{a_1}\right)$	Magnetomotive force
$EP2 = \frac{Np}{2}\left(I_{a_{02}} + i_{a_2}\right)$	Magnetomotive force
$ES = Nsi_s$	Magnetomotive force
$H_{c_1} l_{c_1} + H_{c_3} l_{c_3} = EP1 - EP2$	Ampère's theorem
$H_{c_2}\left[l_{c_2} + \frac{l_g}{\lambda_g}\frac{\mu_{c_2}}{\mu_0}\right] - H_{c_3} l_{c_3} = ES$	Ampère's theorem

$\varphi_{c_1} = \mu_{c_1} H_{c_1} A_{c_1}$	Magnetic flux
$\varphi_{c_2} = \mu_{c_2} H_{c_2} A_{c_2}$	Magnetic flux
$\varphi_{c_3} = \mu_{c_3} H_{c_3} A_{c_3}$	Magnetic flux
N_p	Number of turns of the primary winding
N_s	Number of turns of the secondary winding
R_p	Resistance of the primary winding
R_s	Resistance of the secondary winding
ρ	Internal resistance of the sources
$V_{p_1} - \frac{N_p}{2}\frac{d\varphi_{c_1}}{dt} = \left[\frac{R_p}{2} + \rho\right]\left[I_{a_{01}} + i_{a_1}\right]$	Ohm and Lenz's laws
$V_{p_2} - \frac{N_p}{2}\frac{d\varphi_{c_1}}{dt} = \left[\frac{R_p}{2} + \rho\right]\left[I_{a_{02}} + i_{a_2}\right]$	Ohm and Lenz's laws
$-N_s\frac{d\varphi_{c_2}}{dt} = \left[R_L + R_s\right] i_s$	Ohm and Lenz's laws

4 ESACAP Hessel's Anna amplifier model

Based on the above schematic diagrams and the model of particular components, a complete model has been set-up in the ESACAP network analysis program.

5 Results of simulations

With the above ESACAP model, different simulations can be performed such as:

DC mode, which allows calculating voltage at nodes and current in branches, when no input signal is applied to the amplifier

TRAN mode, which allows calculating in the time domain voltage at nodes and current in branches, when a time dependent signal is applied at the input of the amplifier

PER mode, which allows calculating the harmonic distortion spectrum, at nodes and current in branches, when a sine signal of a given amplitude and frequency is applied at the input of the amplifier

AC mode, which allows calculating the frequency response at nodes and current in branches, when a sine signal of given amplitude is applied at the input of the amplifier.

5.1 DC mode

5.1.1 Voltage at nodes and current in branches

		Measured
V(10):	0.000000E+00	
V(20):	0.000000E+00	
V(30):	7.124598E-01	0,7 V
V(40):	5.839834E-01	
V(60):	3.000000E+02	
V(50):	4.304728E+01	49,4 V
V(70):	5.124307E+01	59,4 V
V(80):	5.124307E+01	
V(11):	5.648684E+01	64,4 V
V(90):	5.593959E+01	
V(31):	3.548687E+02	355,0 V
V(21):	2.103957E+02	212,5 V
V(42):	-1.313391E-01	

V(72):	-1.313391E-01	
V(12):	5.648684E+01	64.4 V
V(32):	3.548687E+02	355,0 V
V(22):	2.103957E+02	216,5 V
V(41):	-1.313391E-01	
V(71):	-1.313391E-01	
V(51):	-1.313391E-01	
V(61):	3.443698E+01	35,0 V
V(52):	-1.313391E-01	
V(62):	3.443698E+01	35,0 V
V(91):	3.545406E+02	
V(92):	3.545406E+02	
V(81):	1.514613E-28	
V(82):	-2.524355E-29	
V(100):	0.000000E+00	
V(110):	0.000000E+00	
I(J10):	4.000000E-03	4,0 mA
I(J20):	8.700000E-03	8,7 mA
I(R10):	0.000000E+00	
I(R20):	0.000000E+00	
I(R30):	5.839834E-03	5,7 mA
I(R40):	5.839834E-03	
I(R50):	5.839834E-03	
I(R60):	0.000000E+00	
I(R70):	0.000000E+00	
I(R80):	0.000000E+00	
I(R90):	5.593959E-05	
I(R11):	4.377970E-03	
I(R21):	4.377970E-03	
I(R31):	-6.167906E-22	
I(R41):	0.000000E+00	
I(R51):	6.913665E-02	
I(R61):	-4.377970E-03	
I(R71):	3.280879E-03	
I(R12):	4.377970E-03	
I(R22):	4.377970E-03	
I(R32):	-6.784696E-21	
I(R42):	0.000000E+00	
I(R52):	6.913665E-02	
I(R62):	-4.377970E-03	
I(R72):	3.280879E-03	
I(Eb10):	-9.839834E-03	
I(Eb11):	-7.351462E-02	
I(Eb12):	-7.351462E-02	

Remark

In the above list:
Voltage at nodes are referred to the ground (Node 0).
Red lines correspond to parameters where measured values are available, as indicated in the Hessel Haagsma PEOHH Project 2013-V4 drawing.
No mention is made, for measured voltages at particular nodes, of the node to which they are referred.

5.1.1 Operating conditions for each tube

From the voltage at nodes and current in branches, we can define, for each tube, their operating points. We have:

First triode type ECC88

$V_{ak_0} = V(50) - V(30) =$ 42,34 V

$V_{gk_0} = V(20) - V(30) =$ -0,71 V

$I_{a_0} = I(R50) =$ 5,84 mA

Second triode type ECC88

$V_{ak_0} = V(60) - V(70) =$ 248,76 V

$V_{gk_0} = V(50) - V(70) =$ -8,19 V

$I_{a_0} = I(J10) =$ 4,00 mA

First triode type 6CG7

$V_{ak_0} = V(21) - V(11) =$ 153,90 V

$V_{gk_0} = V(70) - V(11) =$ -5,25 V

$I_{a_0} = I(R21) =$ 4,38 mA

Second triode type 6CG7

$V_{ak_0} = V(22) - V(12) =$ 153,90 V

$V_{gk_0} = V(80) - V(12) =$ -5,25 V

$I_{a_0} = I(R22) =$ 4,38 mA

First beam tetrodes type KT88

$V_{ak_0} = V(31) - V(61) =$ 320,43 V

$V_{gk_0} = V(51) - V(61) =$ -34,57 V

$I_{a_0} = I(R51) =$ 69,13 mA

Second beam tetrodes type KT88

$V_{ak_0} = V(32) - V(62) =$ 320,43 V

$V_{gk_0} = V(52) - V(62) =$ -34,57 V

$I_{a_0} = I(R52) =$ 69,13 mA

5.2 TRAN mode

The TRAN mode has been used to determine the maximum input voltage before clipping. For this simulation, a sine input signal, having a frequency of 1 kHz, has been chosen.
The grid to cathode voltage for each tube must stay less than or equal to zero.
Corresponding voltages are:

V(20,30)	For the first triode type ECC88
V(50,70)	For the second triode type ECC88
V(70,11)	For the first triode type 6CG7
V(80,12)	For the second triode type 6CG7
V(51,61)	For the first beam tetrodes typeKT88
V(52,62)	For the second beam tetrodes type KT88

Results, when clipping happens, are given on the following graphs.

5.2.1 Driver section (Triode type ECC88 and 6CG7)

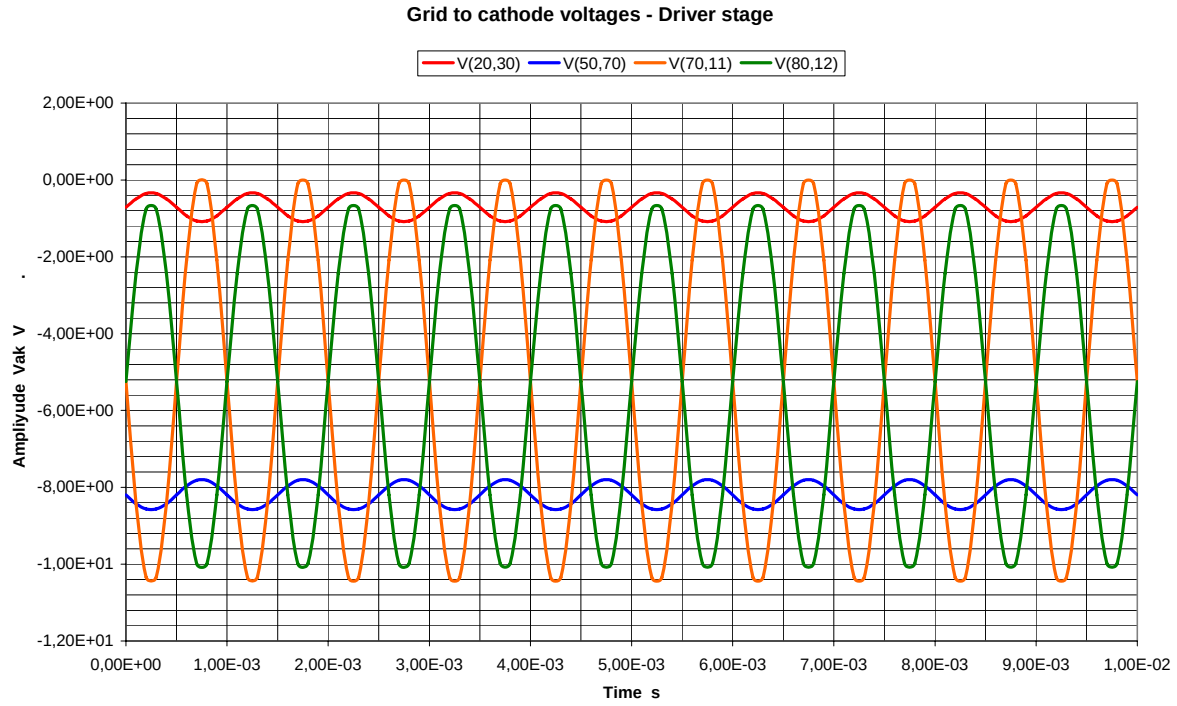

The graph, shows that clipping happens first, on the triode type 6CG7 of the left channel of the phase splitter V(70,11). In this case, the sine input signal has a peak amplitude of: $V_{in\ \ peak} = 0{,}40$ V.

5.2.2 Power section (Beam tetrodes type KT88)

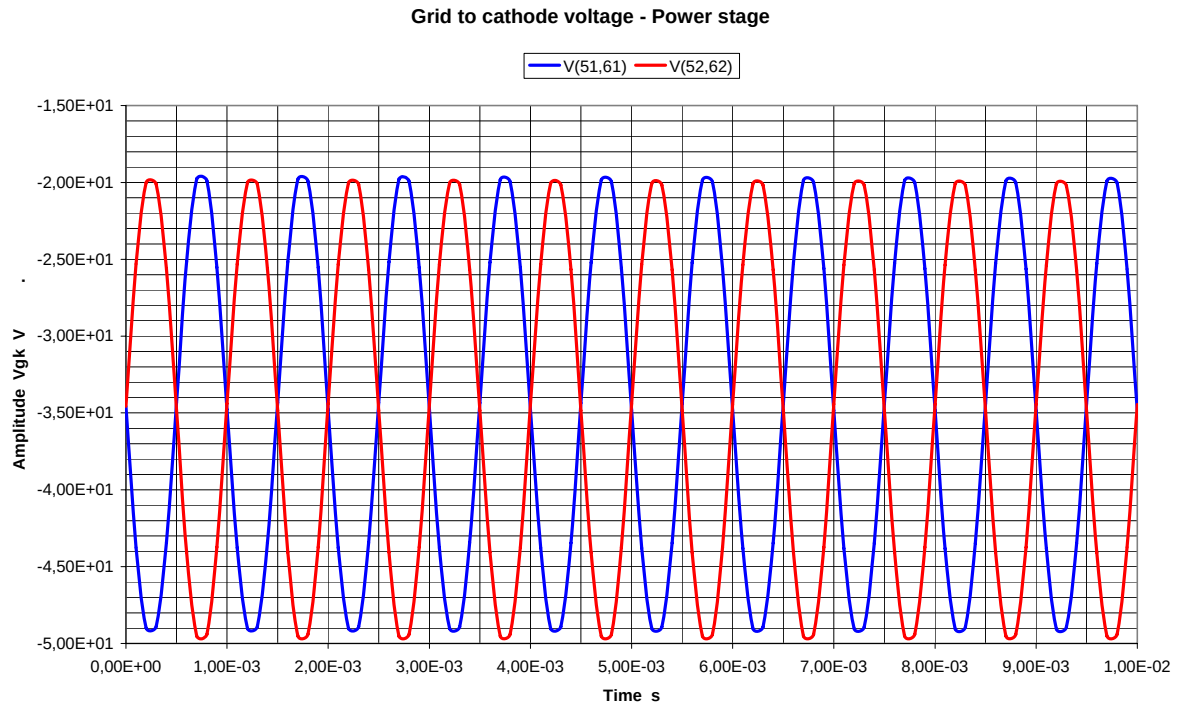

The graph shows that the beam tetrodes type KT88, triode connected, are far away from clipping.

5.2.3 Maximum output on the load

The TRAN mode can also be used to determine the maximum output signal, using the maximum input signal, as defined in the above sections. The corresponding output voltage V(110) is shown on the following graph:

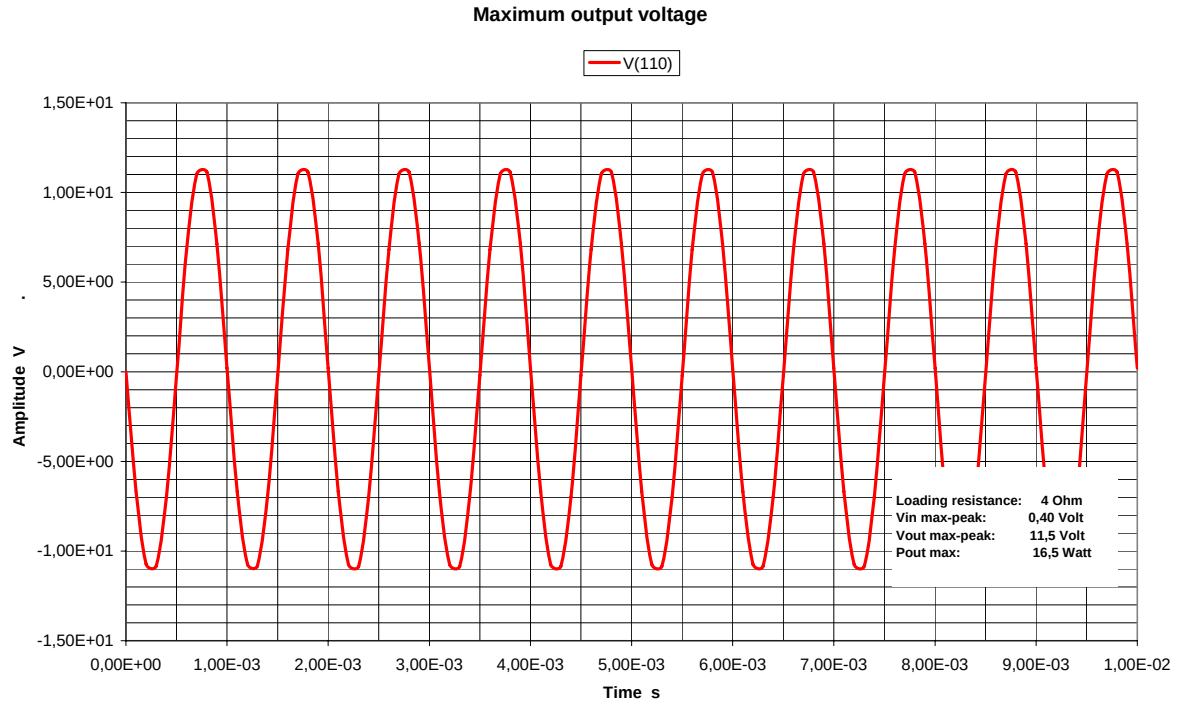

The maximum output power, with a sine input signal, having a peak amplitude of 0,40 V and a frequency of 1 kHz, is of the order of 16,5 W, for a loading resistance of 4 Ohm.

5.3 PER mode

The PER mode allows evaluating, for a sine input signal of given amplitude and frequency, the harmonic distortion spectrum. The graph below shows the harmonic distortion in dB, for a sine input signal at 1 kHz, as a function of the peak amplitude of the input signal.

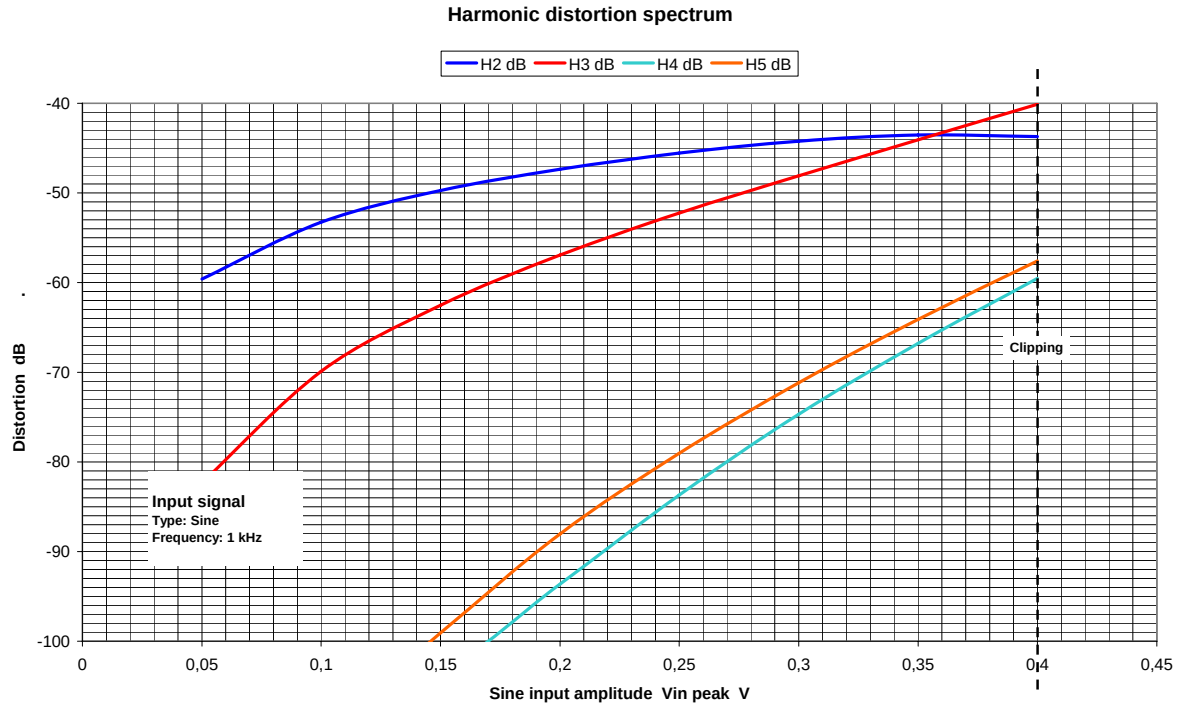

The global figure of the distortion spectrum is dominated by the harmonic 2, at low and medium levels and by the harmonic 3, at high level. The spectrum structure is stable.

5.4 AC mode

The AC mode allows evaluating, the frequency response (Module and Argument) at nodes of interest.

5.4.1 Phase splitter outputs (Nodes 51 and 52)

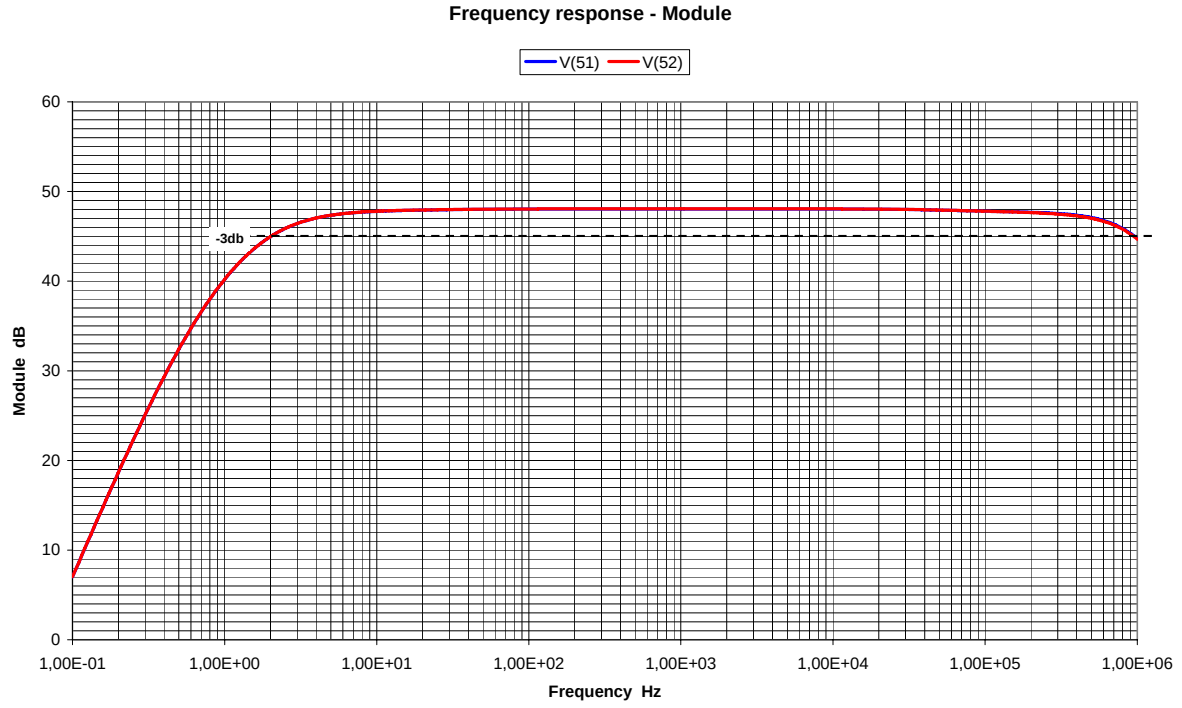

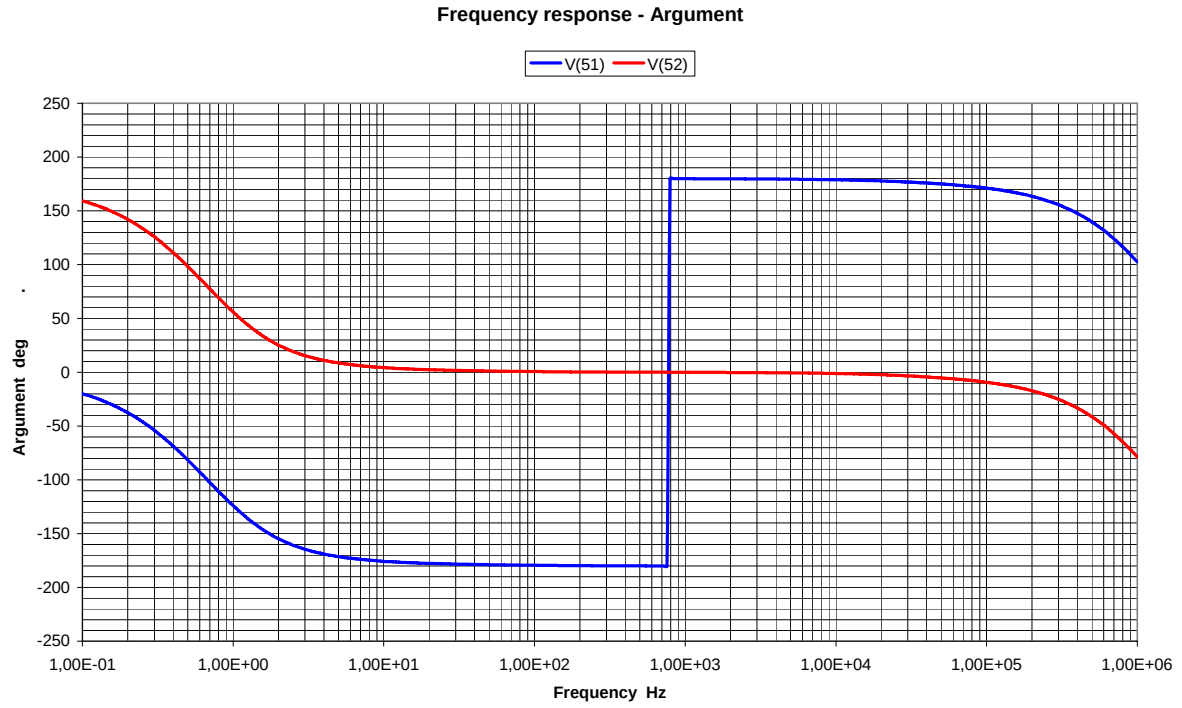

Nodes 51 et 52 are the Left and Right outputs of the driver section. Voltages are referrd to ground (node 0). Both graphs show:

An excellent symmetry between channels

A stable phase difference of 180° between channels
An identical and extremely extended bandwidth for each channel

5.4.1 Power stage output (Node 110)

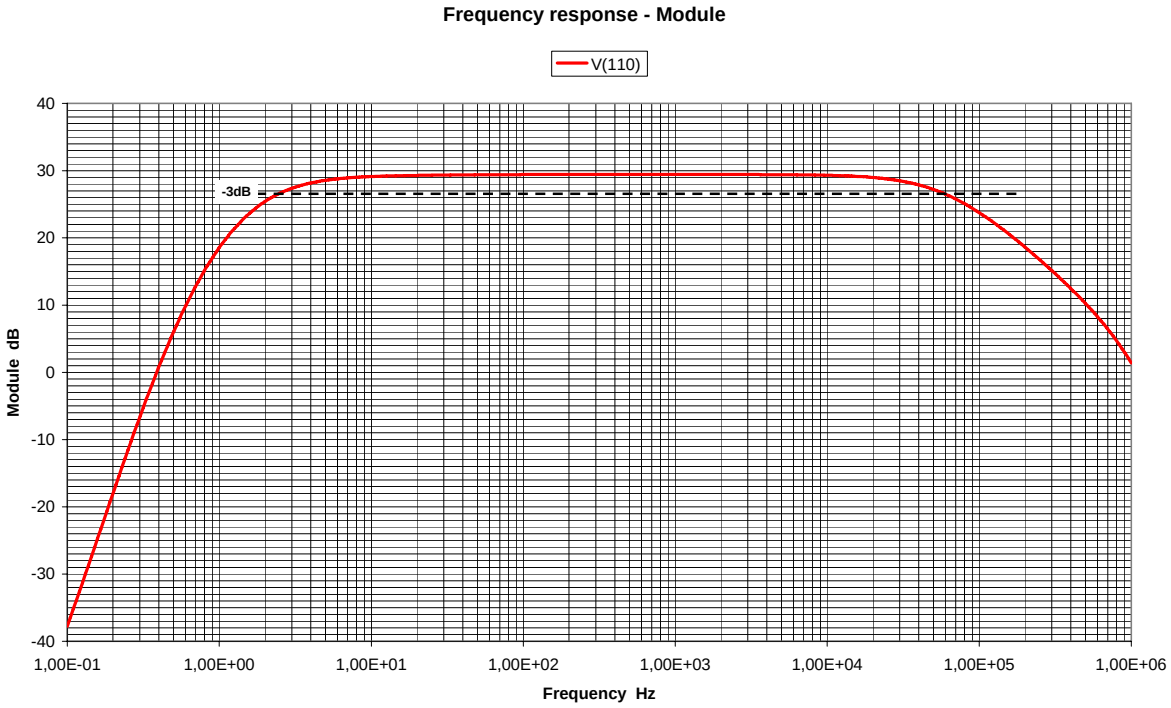

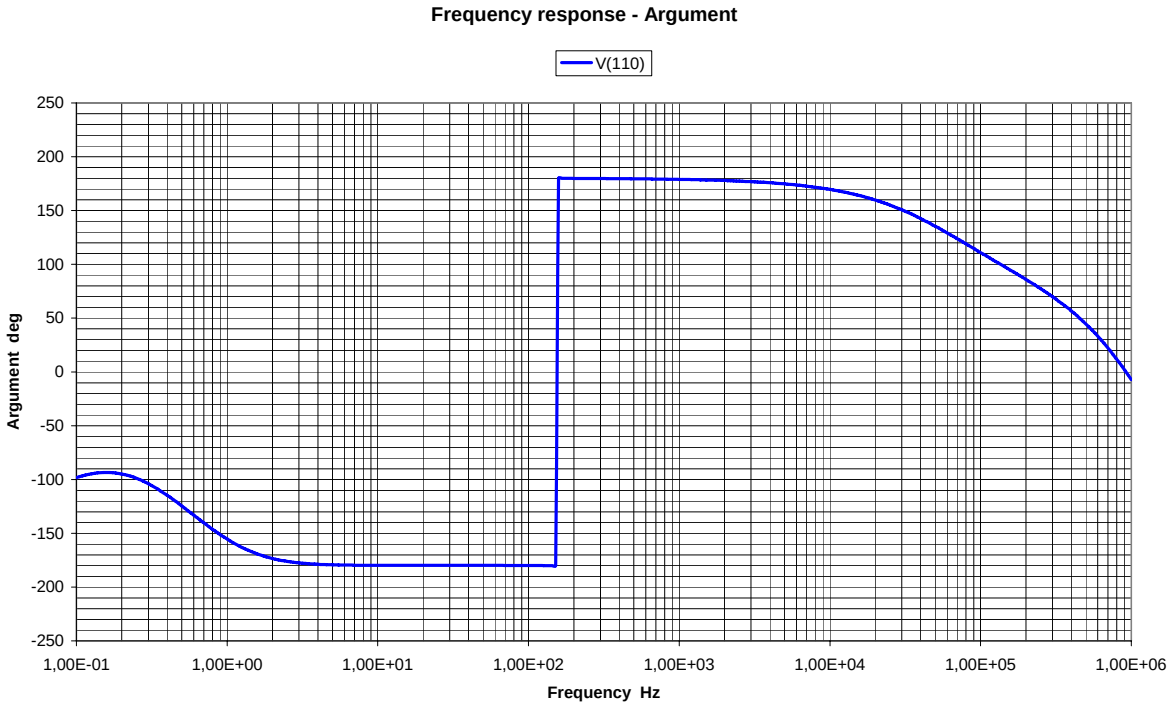

The voltage at node 110 represents the output of the power stage. The voltage is referred to ground (node 0).
Above graphs show:

A large bandwidth ranging from 2,5 Hz up to 60 kHz at -3 dB
A phase varying slowly and continuously, through-out the audio bandwidth

Remark

The response at the high frequency end could be slightly affected by the exact value of the stray capacitance across the primary winding of the OPT and the exact value of the leakage inductance of the OPT, that have been estimated in our analysis.

6 Comments

Results derived from the simulations described in the above sections confirm the excellent sounding impression felt during the amplifiers contest. Nevertheless the following points have drawn our attention. They are:

6.2 Driver section

6.2.1 First stage

The first triode type ECC88 is weakly biased (Vgko=-0,70 Volt) and in the range (0, -1 Volt) where, it is known that the grid current starts to built up, despite the grid stays negative. A higher bias would have been preferable like Vgko=-2 Volt, offering then, a better protection against this phenomena as well as a better dynamic for the input signal.

6.2.2 Second stage

The second triode type EC88 is working as a cathode follower. This choice is surprising as it provides no voltage gain. A direct connection between the first stage and the phase splitter would have been an equivalent but, much simpler solution.

6.2.3 Phase splitter

The phase splitter is of the long tail type and works nicely. This result is due to the current source in the tail.
This stage is the one which limits the input voltage supplied to each channel of the power stage. Many designers are not in favour, using constant current source because finding the resulting sounding not satisfying.

6.1 Power stage

The power stage is a parallel push-pull which requires a subtle network and 2 floating HT supplies. Each tube sees one half of the load in its plate circuit and the other half in its cathode one. The large capacitor, on the filtering section of each supply, allows, in AC condition, connecting the plate to one half of the load and is consequently, an extremely critical component of this circuit.
These large capacitors, of the electrochemical type, are generally rather bad capacitors in AC condition and, if no care is taken, can damage seriously the expected good sounding and performances of the amplifier.
The ESACAP model describes both floating HT supplies as ideal voltage sources which behave in AC condition, as short circuits. Hence, the model assumes an ideal behaviour of these capacitors which is not true.
An alternative solution is making these capacitors using different types of capacitors in parallel having each their specific frequency domain of excellence and to combine them in such way that on the whole Audio band the resulting capacitor works as an ideal one.
This solution is nevertheless not as easy as it seems because, requiring experimenting different brands of capacitors along with long and tedious listening sessions. But, it is the price to pay to bring this excellent amplifier to the level of excellence.

7. Conclusion

In this analysis, we have established and justified a detailed model of the Hessel's Anna amplifier, in the ESACAP network analysis program. All the classical performances of this amplifier have been estimated through different simulations performed using the ESACAP model. All these performances confirm the quality and good sounding noticed during the amplifiers contest at the Menno van der Veen new laboratory. Some points have been raised, that should be revisited in details for clarification, in order to open the door to improvements of this already excellent Audio amplifier.